Electronic Supplementary Material (ESI) for Journal of Materials Chemistry C.
This journal is © The Royal Society of Chemistry 2017

Supporting Information

Optical Properties and Raman-Active Phonon Modes in Two-Dimensional Honeycomb Zintl Phases

M. Q. Arguilla, N. D. Cultrara, M. R. Scudder, S. Jiang, R. D. Ross and J. E. Goldberger*

[1]Department of Chemistry and Biochemistry, The Ohio State University, Columbus, Ohio 43210-1340, United States

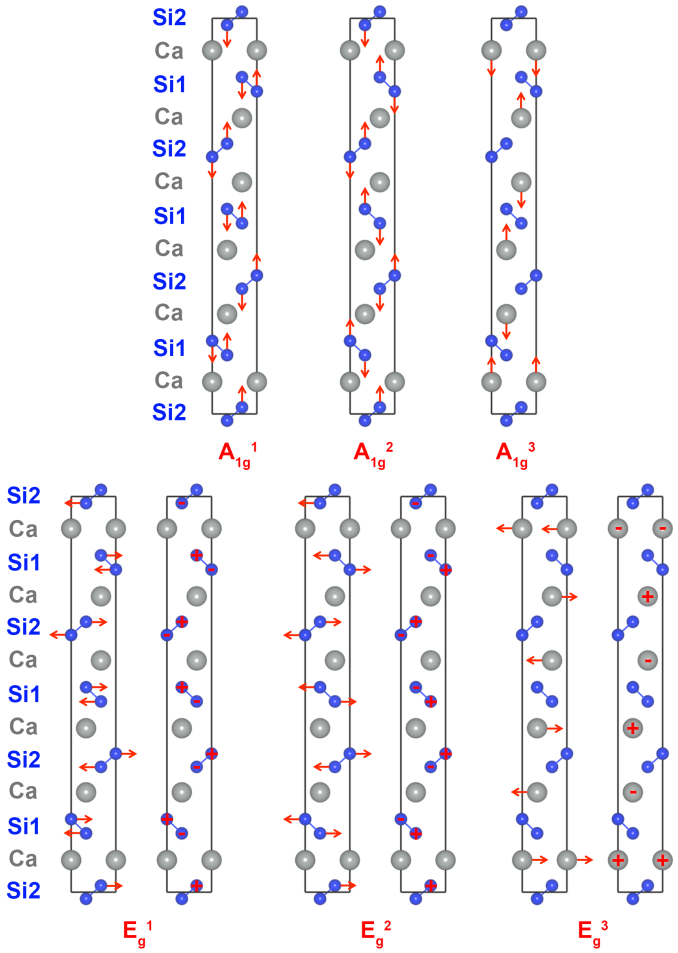

Figure S1. Atom displacements for the out-of-plane (A_{1g}^{1-3}) and in-plane (E_g^{1-3}) Raman vibrational modes of $CaSi_2$.

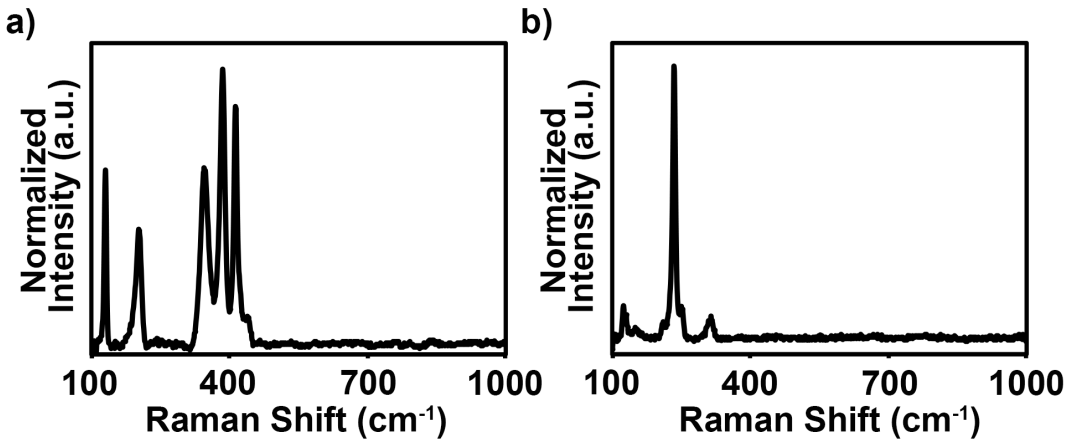

Figure S2. Unpolarized Raman spectra of 6R-layered Zintl phases, (a) $CaSi_2$, (b) $CaGe_2$, showing both the in-plane and out-of-plane Raman modes.

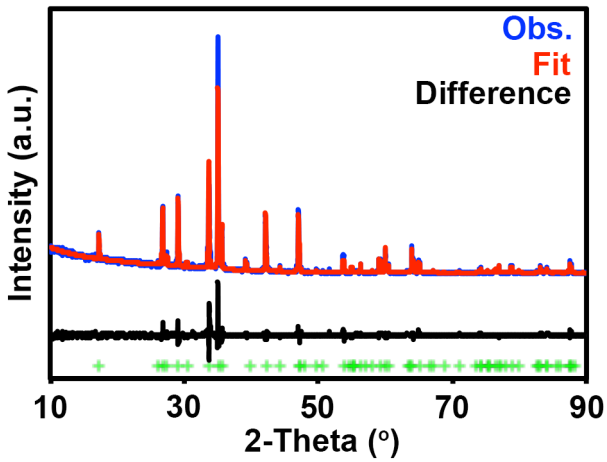

Figure S3. Powder XRD Rietveld refinement results for $CaSi_2$ using TOPAS. The green cross marks correspond to the Bragg reflections of $CaSi_2$.

Table S1. Crystal Data and Refinement Results for $CaSi_2$

$CaSi_2$	Cu $K_{\alpha1}$ radiation
R-3m (No. 166)	λ = 1.5406 Å
a/b = 3.855(8)	2ϑ = 10 - 90
c = 30.65(6)	*T* = 298 K
α/β = 90°	
γ = 120°	
V = 394.6(2)	
R_p/R_{wp} = 3.87/5.99(%)	

Table S2. Fractional atomic coordinates and isotropic displacement parameters based on the refined $CaSi_2$ structure.

Atom	Wyckoff Position	x	y	z	B_{eq} (Å^2)
Ca	6c	0	0	0.080(11)	0.75(2)
Si	6c	0	0	0.346(14)	0.99(2)
Si	6c	0	0	0.181(15)	0.99(2)

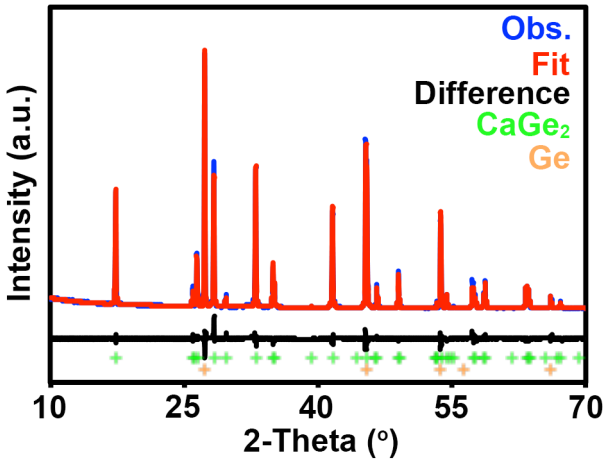

Figure S4. Powder XRD Rietveld refinement results for β-$CaGe_2$ using TOPAS. The phase fraction of Ge was refined to be 24 %. The green and orange cross marks correspond to the Bragg reflections of $CaGe_2$ and Ge, respectively.

Table S3. Crystal Data and Refinement Results for $CaGe_2$

$CaGe_2$	Cu $K_{\alpha1}$ radiation
R-3m (No. 166)	λ = 1.5406 Å
a/b = 3.985(2)	2ϑ = 10 - 70
c = 30.63(2)	T = 298 K
$\alpha/\beta = 90^o$	
$\gamma = 120^o$	
V = 421.2(5)	
R_p/R_{wp} = 2.64/4.13 (%)	

Table S4. Fractional atomic coordinates and isotropic displacement parameters based on the refined $CaGe_2$ structure.

Atom	Wyckoff Position	x	y	z	B_{eq} (Å^2)
Ca	6c	0	0	0.083(1)	0.72(8)
Ge	6c	0	0	0.1827(0)	0.38(7)
Ge	6c	0	0	0.3496(6)	0.38(7)

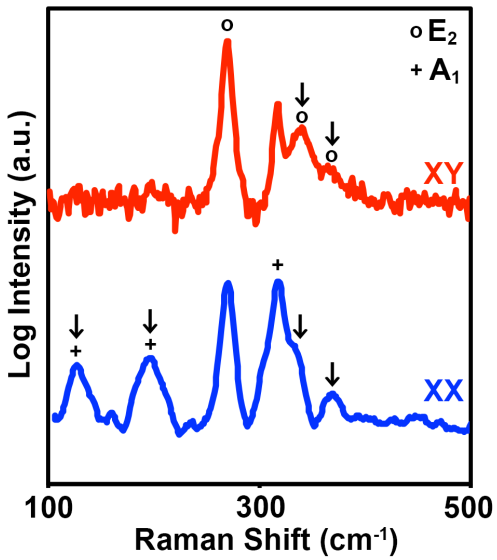

Figure S5. Logarithmic plot of the co- and cross-polarized NaSnP Raman spectra highlighting the weak Raman modes in the spectra (arrows).

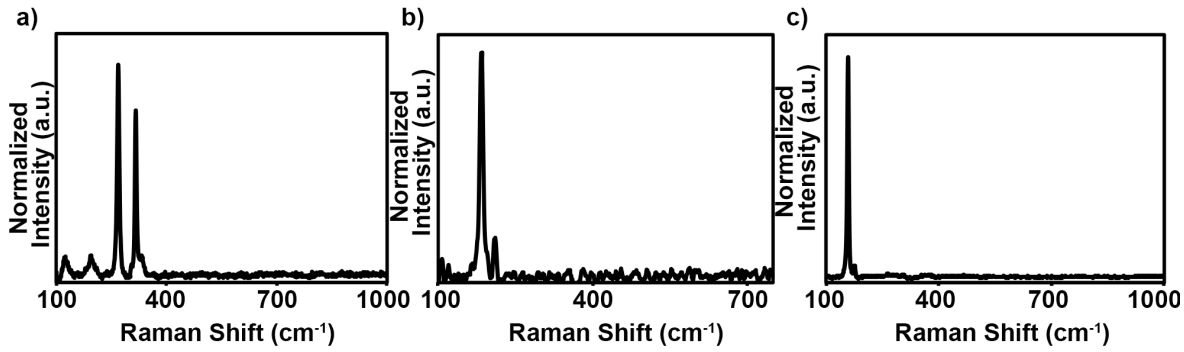

Figure S6. Unpolarized Raman spectra of 2H-layered Zintl phases, (a) NaSnP, (b) KSnAs and (c) KSnSb, showing both the in-plane and out-of-plane Raman modes.

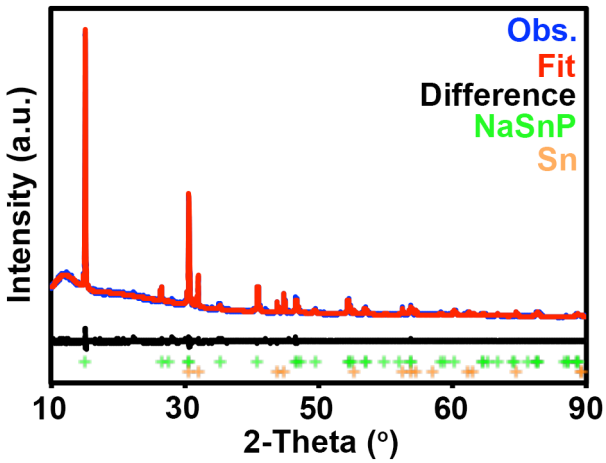

Figure S7. Powder XRD Rietveld refinement results for NaSnP using TOPAS. The phase fraction of Sn was refined to be 15.9 %. The green and orange cross marks correspond to the Bragg reflections of NaSnP and Sn, respectively.

Table S5. Crystal Data and Refinement Results for NaSnP.

NaSnP	Cu $K_{\alpha1}$ radiation
$P6_3mc$ (No. 186)	λ = 1.5406 Å
a/b = 3.882(12)	2ϑ = 10 - 90
c = 11.68(3)	T = 298 K
α/β = 90°	
γ = 120°	
V = 152.4(11)	
R_p/R_{wp} = 3.54/4.74(%)	

Table S6. Fractional atomic coordinates and isotropic displacement parameters based on the refined NaSnP structure.

Atom	Wyckoff Position	x	y	z	B_{eq} (Å^2)
Na	2b	1/3	2/3	0.281(11)	1.3(3)
P	2a	1/3	2/3	0.614(11)	0.92(3)
Sn	2b	0	0	0	0.080(4)

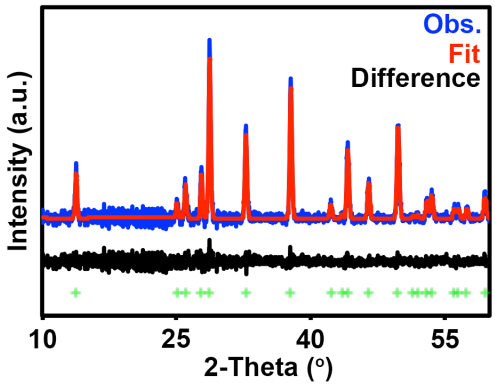

Figure S8. Powder XRD Le Bail fitting results for KSnAs using TOPAS. The green cross marks correspond to the Bragg reflections of KSnAs.

Table S7. Crystal Data and Le Bail Fitting results for KSnAs.

KSnAs	Cu $K_{\alpha1}$ radiation
$P6_3mc$ (No. 186)	λ = 1.5406 Å
a/b = 4.100(3)	2ϑ = 10 - 60
c = 12.824(1)	T = 298 K
α/β = 90°	
γ = 120°	
V = 186.74(1)	
R_p/R_{wp} = 5.01/6.57(%)	

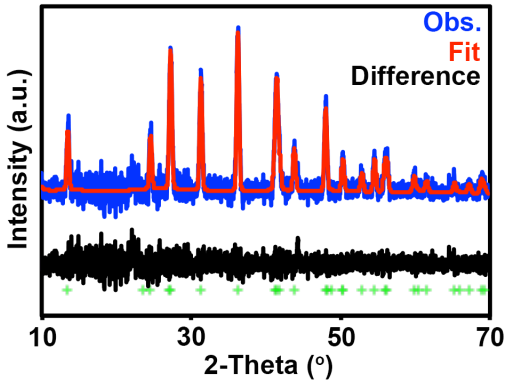

Figure S9. Powder XRD Le Bail fitting results for KSnSb using TOPAS. The green cross marks correspond to the Bragg reflections of KSnSb.

Table S8. Crystal Data and Le Bail Fitting results for KSnSb.

KSnSb	Cu $K_{\alpha1}$ radiation
$P6_3mc$ (No. 186)	λ = 1.5406 Å
a/b = 4.352(6)	2ϑ = 10 - 70
c = 13.14(2)	T = 298 K
α/β = 90°	
γ = 120°	
V = 215.7(6)	
R_p/R_{wp} = 7.14/9.54(%)	

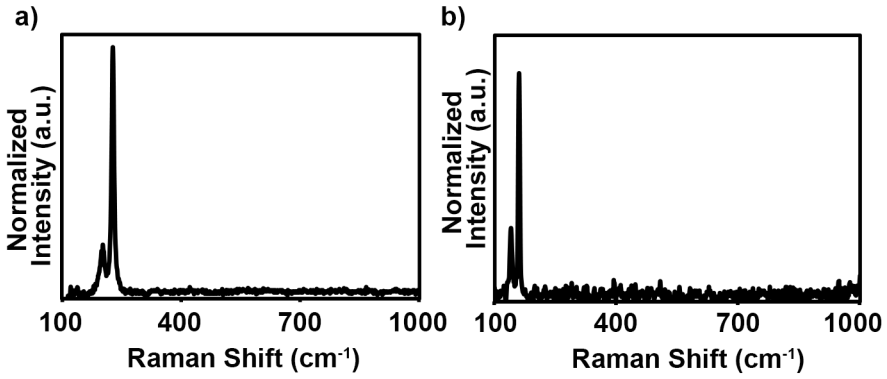

Figure S10. Unpolarized Raman spectra of 1T-layered Zintl phases, (a) $EuGe_2$ and (b) $BaSn_2$, showing both the in-plane and out-of-plane Raman modes.

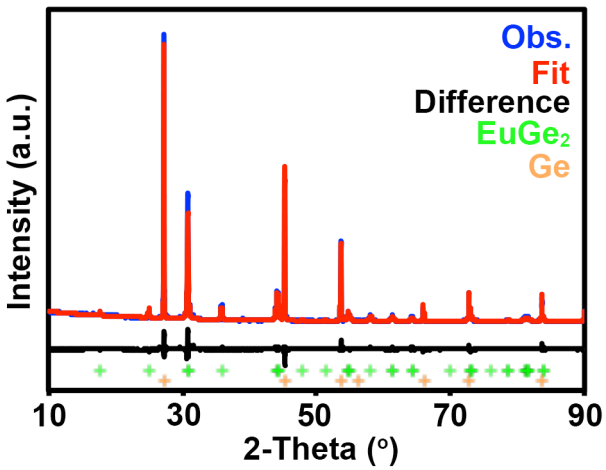

Figure S11. Powder XRD Rietveld refinement results for $EuGe_2$ using TOPAS. The phase fraction of Ge was refined to be 10.6 %. The green and orange cross marks correspond to the Bragg reflections of $EuGe_2$ and Ge, respectively.

Table S9. Crystal Data and Refinement Results for $EuGe_2$.

$EuGe_2$	Cu $K_{\alpha1}$ radiation
P-3m1 (No. 164)	λ = 1.5406 Å
a/b = 4.102(3)	2ϑ = 10 - 90
c = 4.999(4)	T = 298 K
α/β = 90°	
γ = 120°	
V = 72.84(1)	
R_p/R_{wp} = 3.86/5.51(%)	

Table S10. Fractional atomic coordinates and isotropic displacement parameters based on the refined $EuGe_2$ structure.

Atom	Wyckoff Position	x	y	z	B_{eq} (Å^2)
Eu	1a	0	0	0	0.040(3)
Ge	2d	1/3	2/3	0.398(7)	0.39(3)

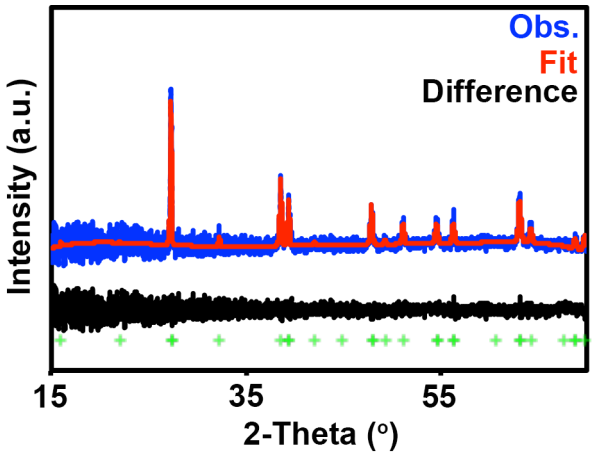

Figure S12. Powder XRD Rietveld refinement results for $BaSn_2$ using TOPAS. The green cross marks correspond to the Bragg reflections of $BaSn_2$.

Table S11. Crystal Data and Refinement Results for $BaSn_2$.

$BaSn_2$	Cu $K_{\alpha1}$ radiation
P-3m1 (No. 164)	λ = 1.5406 Å
a/b = 4.660(2)	2ϑ = 15 - 70
c = 5.539(3)	T = 298 K
α/β = 90°	
γ = 120°	
V = 104.2(1)	
R_p/R_{wp} = 4.60/6.34(%)	

Table S12. Fractional atomic coordinates and isotropic displacement parameters based on the refined $BaSn_2$ structure.

Atom	Wyckoff Position	x	y	z	B_{eq}(Å^2)
Ba	1a	0	0	0	0.072(3)
Sn	2d	1/3	2/3	0.398(5)	0.083(3)

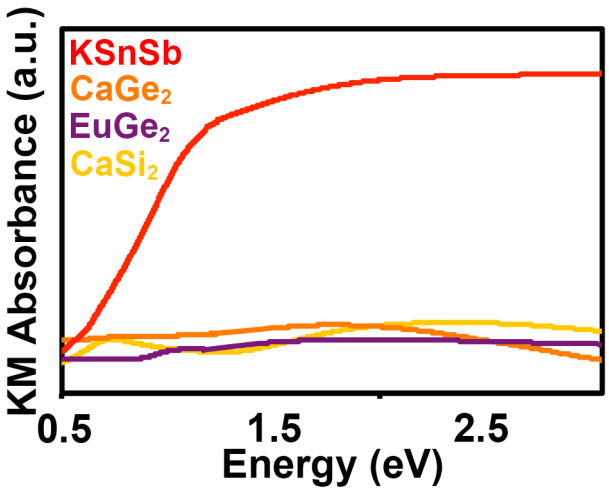

Figure S13. Kubelka-Munk diffuse reflectance spectra of metallic Zintl phases showing the broadband absorption across the visible and near-infrared range. The absorbance spectrum of KSnSb was included for reference.

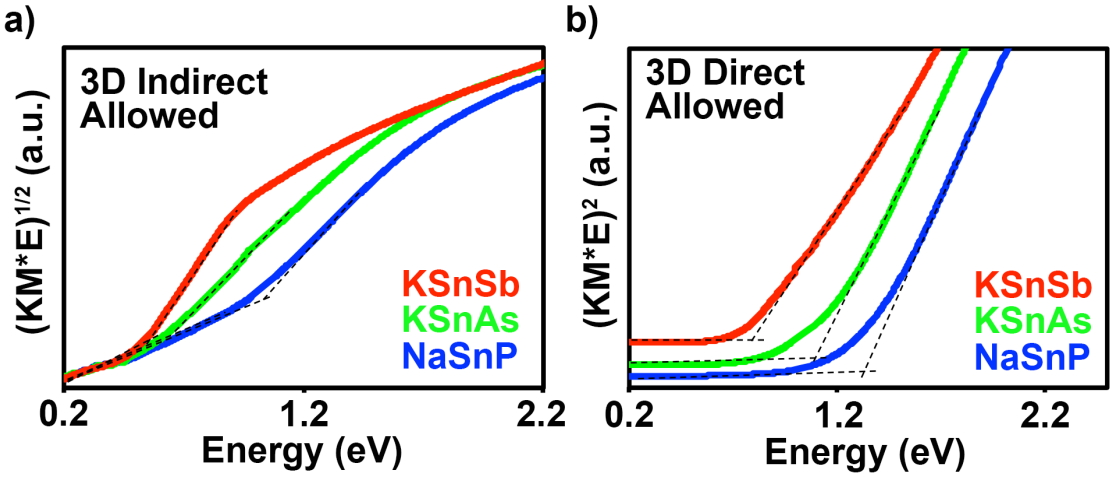

Figure S14. Diffuse reflectance absorbance spectra of semiconducting Zintl phases fitted using the Tauc-Davis-Mott models of 3D densities of states of (a) 3D indirect allowed, (b) 3D direct allowed transitions.

Table S13. Summary of optical transitions obtained from the Tauc-Davis-Mott models for semiconducting layered Zintl phases under study.

Phase	3D Direct Allowed (eV) $(\hbar\omega - E_g)^2$	3D Indirect Allowed (eV) $(\hbar\omega - E_g' \pm E_p)^{1/2}$
NaSnP	1.28	0.95 ± 0.033
KSnAs	0.97	0.65 ± 0.023
KSnSb	0.80	0.54 ± 0.020